



National
Defence

Défense
nationale



SPACE RADIATION ENVIRONMENT ESTIMATION FOR RADARSAT II

by

L. Varga, G.T. Pepper and P. Woods

19961113 083

[DTIC QUALITY INSPECTED 2]

DEFENCE RESEARCH ESTABLISHMENT OTTAWA
REPORT NO. 1292

Canada

July 1996
Ottawa

DISTRIBUTION STATEMENT A

Approved for public release;
Distribution Unlimited



National Défense
Defence nationale

SPACE RADIATION ENVIRONMENT ESTIMATION FOR RADARSAT II

by

L. Varga and G.T. Pepper
Space Systems and Technology Section

and

P. Woods
CSA/RADARSAT Program Office

DEFENCE RESEARCH ESTABLISHMENT OTTAWA

REPORT NO. 1292

PCN
1410 SS-05E03

July 1996
Ottawa

ABSTRACT

Estimation of the radiation environment for RADARSAT II satellite (to be launched in the fall 2000) is presented using industry-standard space radiation models CREME and AE8/AP8. Radiation transport Monte Carlo codes TRIM and ITS 3.0 Tiger were then subsequently used to calculate the total radiation dose received by RADARSAT II during the planned 5.25 year mission.

RÉSUMÉ

L'estimation de l'environnement de radiation du satellite RADARSAT II (à être lancé à l'automne de l'an 2000) est présenté, utilisant les standards industriels de modèle de radiation spatiale CREME et AE8/AP8. Les codes Monte Carlo de transport de radiation TRIM et ITS 3.0 TIGER étaient alors subséquemment utilisés pour calculer la dose totale de radiation reçue par RADARSAT II durant la mission planifiée de 5.25 ans.

EXECUTIVE SUMMARY

One of the aspects of the engineering project when developing a space-based platform, should also involve a task to estimate the mission-specific radiation environment. In view of the investment involved, it is vital that such information becomes available ahead of the design stage of the project. Subsequently, a selection of proper materials, coatings and electronic components can be made to ensure that the space system will be able to withstand the radiation environmental rigours encountered in orbit for the duration of the planned mission.

The work presented in this report forms a part of an on-going effort at DREO to develop a methodology that enables the space system designers to obtain mission-specific total radiation dose evaluation. Specifically, it is a summary of a task commissioned by CSA to obtain the best estimate of the space radiation environment for the RADARSAT II satellite. The method exploits utilization of space radiation environmental models such as CREME, AE-8 and AP-8. Details of these models are described. In addition, we have employed radiation transport codes, such as TRIM and ITS 3.0 Monte Carlo code to model electrons/photons effects and PROTDose, developed at DREO, to calculate the total radiation dose received by the RADARSAT II during the planned 5.25 year mission.

CONTENTS

<u>ABSTRACT</u>	iii
<u>RÉSUMÉ</u>	iii
<u>EXECUTIVE SUMMARY</u>	v
<u>CONTENTS</u>	vii
1. Introduction	1
2. Mission Data	1
3. Models	2
3.1 Space Environment Codes	2
3.2 Radiation Transport Codes	3
3.2.1 Electron Depth/Dose Computation	3
3.2.2 Proton Depth/Dose Computation	4
4. Results	5
4.1 Electron Environment	5
4.2 Proton Environment	6
4.3 Heavy ions	10
5. Mission Dose Determination	12
5.1 Electron Depth/Dose Distribution	12
5.2 Proton Contribution to Total Mission Dose	13
5.3 He Contribution to Total Mission Dose	19
6. Summary.....	21
7. References	23

1. INTRODUCTION

Earth-orbiting spacecrafts are subjected to the deleterious effects of ionizing radiation on electronics. The type, energy and fluence of ionizing radiation encountered during the mission primarily depend upon the spacecraft's orbital parameters and the solar activity occurring during the mission. The orbit of a spacecraft, due to relatively well structured spatial distribution of the geomagnetically-trapped radiation, determines to what type of radiation environment a spacecraft will be subjected over the course of the mission. Solar activity produces transient variation in the radiation flux that can significantly affect the lifetime of electronic and other systems on-board of the spacecraft.

Ionizing radiation adversely affects many semiconductor devices comprising the electronic systems on-board of the spacecraft^(1,2). The problem is exacerbated as the "critical" or "sensitive" volume of semiconductor devices continue to shrink, as device feature sizes become progressively smaller. The effect of interaction of ionizing radiation with semiconductor devices can be classified into three main categories; a) total dose effects, b) displacement damage effects and c) single-event upset (SEU) effects. All three of these effects are of great importance to modern satellite systems; this study is concerned only with the total dose effects.

In order to design a satellite system that can withstand the rigours of the ionizing radiation over a desired mission duration, the space radiation environment and the impact of that environment on the electronic systems must be assessed. Defence Research Establishment Ottawa has conducted such a study (under contract to CSA/RADARSAT Project Office) to determine the best estimate of the radiation environment and the resulting total ionizing radiation dose that will be encountered by RADARSAT II.

2. MISSION DATA

The following information, supplied by the RADARSAT Program Office, has been utilized to estimate the space radiation environment for the RADARSAT II satellite.

Orbit: semi-major axis = 7172.655025 km;
eccentricity = 0.00114836;
inclination = 98.5784 degrees;
argument of perigee = 90 degrees;
right ascension of ascending node(degrees)=
-80.8099425+((1-12:00:00)/24 + t/365.24219)x360;
mean anomaly(degrees)=343.24 x (t-t₀ -0.017467134)x360;

Estimated Launch Date: September 2000;
Mission Duration: 5.25 years;
Estimated maximum Al shielding: 3.0cm;

3. MODELS

3.1 SPACE ENVIRONMENT CODES

The AE-8⁽³⁾ trapped radiation model was used to determine the total mission electron flux. The model is applicable to geomagnetically trapped electrons in the energy range from 40 keV to 3.5 MeV with L values ranging from L=1.15 to L=11. The environment model is based on measurements obtained by AZUR, OV1-19, OV3-3, ATS5 and ATS6 spacecraft⁽³⁾. For the RADARSAT mission, coinciding with the maximum solar activity period of the solar cycle #23, the AE-8MAX module of AE-8 was utilized. Another module of AE-8, namely AE-8MIN, relates to solar minimum epochs.

The proton component of the RADARSAT II radiation environment is composed of geomagnetically trapped protons, galactic cosmic ray protons and protons of solar flare origin. The trapped proton flux was estimated using the AP-8 trapped proton model environment. The model is applicable to trapped protons in the energy range from 100 keV to over 1 GeV. Data used to generate AP-8 model have been obtained from a number of satellites⁽⁴⁾. The interested reader may consult the above given reference. AP-8 has two modules, AP-8MAX and AP-8MIN, referring to solar maximum and solar minimum epochs respectively. To use the above models, the satellite's orbit parameters are placed in an input file of the program called "ORBIT". The program converts the satellite's trajectory from R-λ coordinates to B-L coordinate system, since the spectrum of the trapped radiation is conveniently mapped in the B-L coordinates. Both AP-8 and AE-8 use the IGRF 1965 magnetic field model for solar minimum epochs and Hurwitz 1970 model for solar maximum epochs. The program "VETTE" uses the B-L trajectory of the satellite and trapped electron and proton data for solar maximum and solar minimum as "look-up" tables to obtain total radiation flux impinging on the satellite. The output of the program is set by setting appropriate switches (tabcons) in the input file for "VETTE".

The contribution to the total proton flux from galactic cosmic rays and solar flares was obtained using the CREME⁽⁵⁾ model. CREME is composed of several modules to obtain estimates of ion spectra, LET spectra or estimates of the bit-upset rate for a particular semiconductor device in a specific orbit. Additional capabilities of CREME include incorporation of the geomagnetic shielding effect, the Earth-shadowing effect as well as the selection of the so called "Interplanetary Weather Index" (IWI). There are twelve (enumerated one through twelve in the code) interplanetary weather conditions. Three of the weather indices (1,2 and 4 in the CREME model) pertain only to galactic cosmic rays. The other 9 indices (3 and 5 to 12) pertain to combination of solar flare and cosmic rays where the solar flare rays have various intensities and compositions.

In CREME, analytical functions fitted to the observed spectra of protons, He

and Fe provide the base for determining spectra for other elements. For example, for the case of galactic cosmic rays, the alpha spectrum is scaled down by factors ranging from⁽⁵⁾ 3.04×10^{-2} to 2.34×10^{-4} to obtain spectra of elements up to phosphorus. The values of these scaling factors were determined from element-abundance measurements made during the French-Danish experiment⁽⁶⁾ on board HEAO-3. For heavier ions or solar flare spectra, different scaling factors and methods are used⁽⁵⁾.

The contribution from anomalously large solar flares is estimated separately. King's⁽⁷⁾ model have been adopted for this purpose. In the model, a solar cycle is divided into 7 active and 4 quiet years. The Burrell-modified Poisson statistics (equation 1, below) is then applied to obtain confidence levels associated with the occurrence of very large solar flares during the mission of the satellite.

$$P(n, t, N, T) = \sum_{i=1}^n \frac{(1+N)! \left(\frac{t}{T}\right)^i}{i! N! \left(1 + \frac{t}{T}\right)^{1+i+N}} \quad (1)$$

where, n is the number of events over the time period t, and N is the number of expected very large flares over the period T. In King's model, N=1 and T=7 years, based on the solar cycle #21. The solar flare used as standard in King's model is the one that occurred in August 1972. This flare is modelled by CREME by setting IWI=9 or 10, the two differing only in heavy ion abundance. It should be noted that King's model also provides an estimate of the level of confidence for the number of ordinary solar flares, in which case the parameter N is equal to 24 and T remains the same, ie. 7 years.

3.2 RADIATION TRANSPORT CODES

3.2.1 Electron Depth/Dose Computation

The Integrated TIGER Series (ITS), version 3.0, of the time-independent coupled electron/photon Monte Carlo radiation transport code was employed to estimate the electron dose as a function of aluminum shielding depth. The ITS member code TIGER was used to conduct a one-dimensional (i.e. a semi-infinite plane) Monte Carlo simulation of the depth/dose distribution for an arbitrary 2π isotropic electron source energy spectrum.

The TIGER code models the transport of both electrons and photons (including Bremsstrahlung) for electron/photon energies down to 1 keV. The energy deposited (i.e. dose) can be scored in any combination of material(s) as a function of depth. Other member codes in the ITS series can perform both multi-material and multidimensional electron/photon transport, but were not utilized in this work.

3.2.2 Proton Depth/Dose Computation

The calculation of the proton depth/dose profile in Al shielding material was accomplished via the use of two computer codes - the TRAnsport of Ions in Materials (TRIM code⁽⁹⁾) code and the PROTDose code, the latter being developed in-house at Defence Research Establishment Ottawa.

The TRIM code (version TRIM-92) is a three-dimensional Monte Carlo transport code for ions (up to and including 2 GeV/amu) in multi-layered materials. For a given ion species, energy and angle of incidence, TRIM can estimate the energy deposited as a function of depth, for a given target material. TRIM can also produce stopping power and ion range tables for any combination of ion species and target materials.

The application of a state-of-the-art Monte Carlo ion transport code, such as TRIM, to calculate the energy deposited versus depth yields more accurate data than other analytical techniques commonly in use today. For example, SHIELDOSE and other computer codes employ table look-up techniques to assist in the calculation of energy loss by energetic protons in materials. The data contained in these tables are based upon the straight-ahead, continuous-slowning-down approximation (CSDA) for the energy loss by protons. This method yields comparatively good results for relatively thin targets (relative to the range of the ion in the target material), high ion energies and small angles of incidence, however, this is not the case for space shielding calculations. Here the flux is isotropic, the target material (Al shielding) can be considered "thin" to "thick" relative to the ion range and the energy span can be from a fraction of an MeV/amu to many GeV/amu or beyond. The CSDA approximation can yield significant error in the depth/dose data, especially at the end of the ion track, where the statistical nature of energy loss by the ion is most evident. This is where the Monte Carlo technique can provide a distinct advantage in terms of yielding the most accurate results.

For our purposes, for a given proton [or He ion] energy of interest, TRIM simulations were performed to obtain data on energy deposited versus depth in aluminum, for 10 angles of incidence, ranging from 0 to 85 degrees [i.e. 0, 10, 20, 30, 40, 50, 60, 70, 80 and 85 degrees angle of incidence]. This data set was produced for each energy window in the window-integrated energy spectrum. TRIM was also used to generate stopping powers for protons (also He ions) in silicon.

The PROTDose code, developed in-house at Defence Research Establishment Ottawa, uses TRIM-generated Monte Carlo data to compute a depth/dose profile in aluminum for a given ion species (e.g. protons) and window-integrated energy spectrum. For each window energy, PROTDose uses the corresponding TRIM-generated energy deposited versus depth (Al) data, as a function of angle of incidence, to calculate a single depth/dose curve for a 2π isotropic flux.

PROTDOSE accomplishes this by dividing the 2π isotropic flux into 90 (or more) equal solid angles and computing a depth/dose curve for each solid angle. This is done by interpolating data from the 10 energy versus depth deposition curves produced by TRIM, for the various angles of incidence described previously. What results is a single depth/dose curve for each window energy, normalized to one incident ion per 2π isotropic flux. After all the depth dose curves are computed, they are weighted by the appropriate fluence for the given energy window and summed, yielding the mission depth/dose curve.

4.RESULTS

4.1 ELECTRON ENVIRONMENT

The major source of electrons at the RADARSAT II orbit are the Van Allen radiation belts, as shown in Figure 1. There are three main locations where the satellite will encounter trapped electrons, namely: a) The South Atlantic Anomaly (SAA), b) the Auroral Zones of the northern hemisphere and c) the Auroral Zone of the southern hemisphere. The trapped electron flux found at very low altitudes in the vicinity of SAA is caused by the relatively weak magnetic field present in

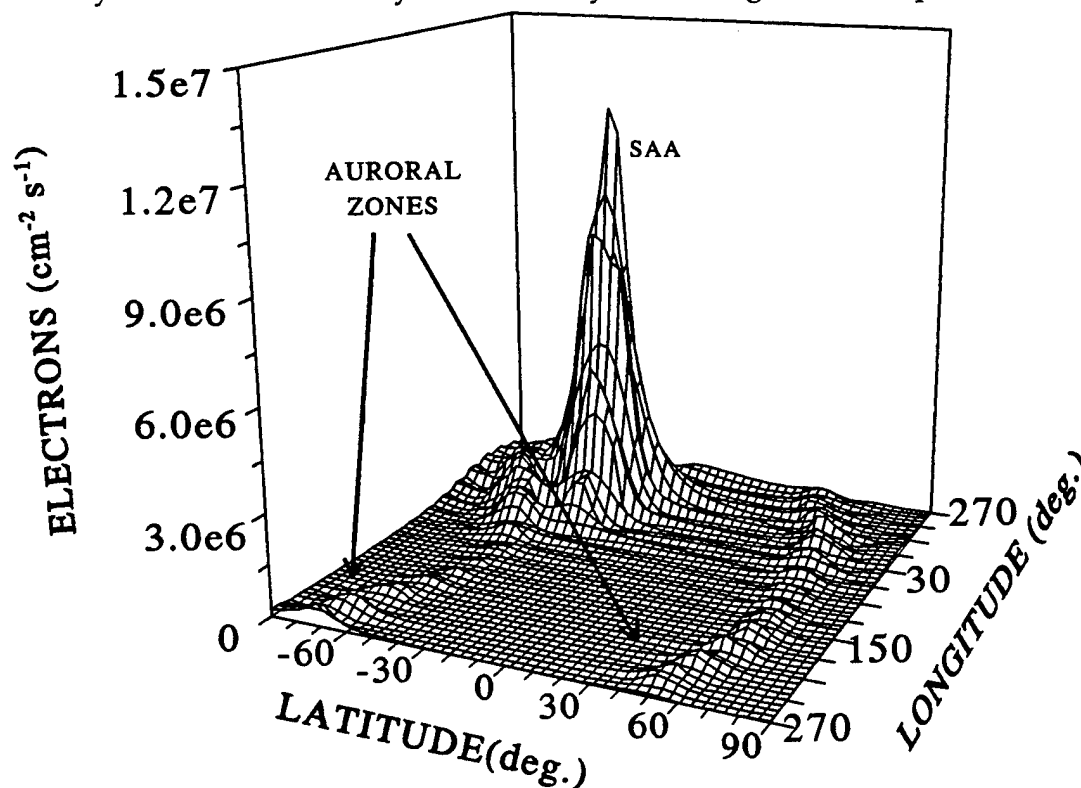


Figure 1. Spatial distribution of trapped electrons at the orbit of RADARSAT II.

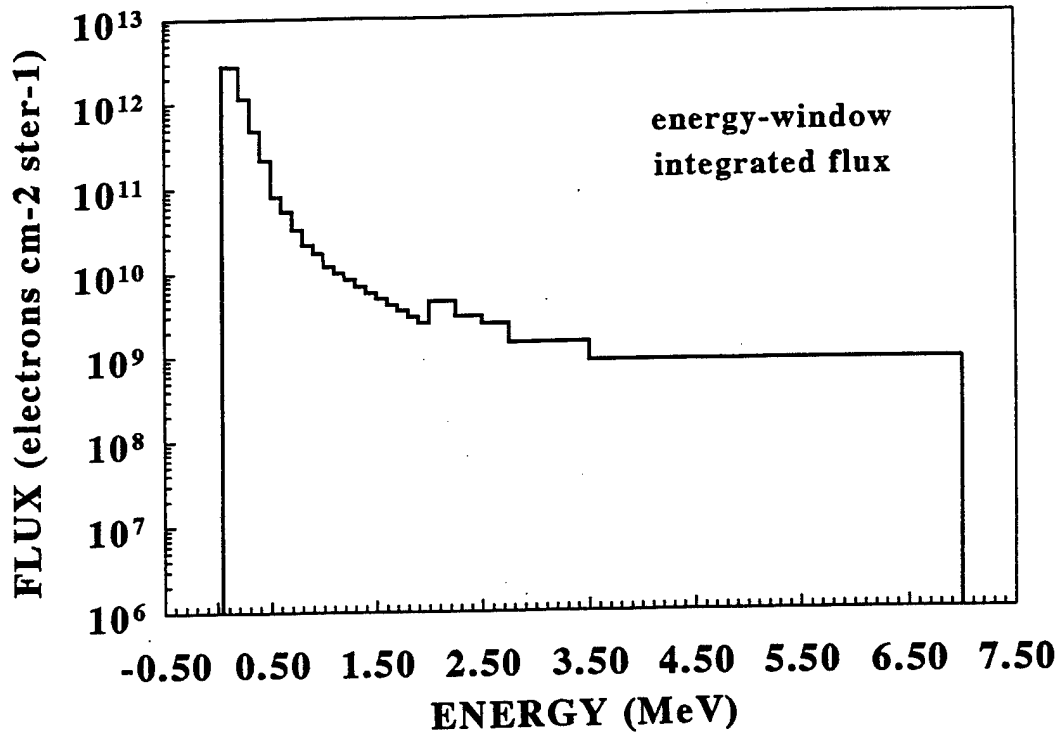


Figure 2. Mission-integrated estimation of electron fluence for RADARSAT II.

that region. The weaker magnetic field causes the magnetic mirror points of trapped electrons to be shifted to altitudes lower than the RADARSAT's orbit. The auroral zone electrons appear in Figure 1 as two bands located above the 50th degree latitude north and south. The origin of these electrons is the outer radiation belts. Figure 2 shows the energy-window integrated electron flux for the RADARSAT II mission; the tabular form of the electron spectrum is given in Table 1.

4.2 PROTON ENVIRONMENT

The major contribution to the trapped proton flux impinging on the skin of RADARSAT will also occur at SAA as shown in Figure 3. The contribution to trapped proton flux from other parts of the orbit trajectory is much less than for trapped electrons. The total accumulated proton spectrum flux from these areas over the mission of the satellite is shown in Figure 4.

The contribution of galactic cosmic ray protons to the total mission flux is also depicted in Figure 4. To obtain the contribution from the galactic cosmic rays to the total proton flux, an IWI=3 was selected. Using this interplanetary weather index, CREME estimates the worst case flux of galactic cosmic rays superimposed by solar activity (flares and corotating solar events such as coronal holes). The curve represents a flux of galactic cosmic ray protons high enough that there is only a 10%

chance of it being surpassed. This spectrum flux differs from the spectrum flux of pure galactic cosmic rays (not shown) also by having a higher flux at the low-energy end of the spectrum. Above approximately 100 MeV, the spectrum is identical with the spectrum of pure galactic cosmic ray protons.

The final contribution to the total-mission proton flux is from anomalously large solar flares. Figure 5 shows the confidence levels of predicting the number of very large solar flares (such as the one that occurred in August 1972) during the RADARSAT mission. The vertical axis represents the confidence levels that the number of flares (shown on the abscissa) will not be exceeded during the mission of RADARSAT II. A 95% confidence limit for RADARSAT II allows for four (4) anomalously large solar flares. In determining the mission proton flux contributed by the anomalously large flares, it was assumed a flare duration to be 4 days long (quoted numbers are from 1 to 5 days⁽⁵⁾). Notably, the trapped proton component and the solar flare proton component are the significant contributors to the total proton flux for the mission. The galactic cosmic ray flux contributes mainly at the high-energy end of the spectrum as shown in Figure 4. Table 2 gives numerical values of individual proton components as well as the total flux.

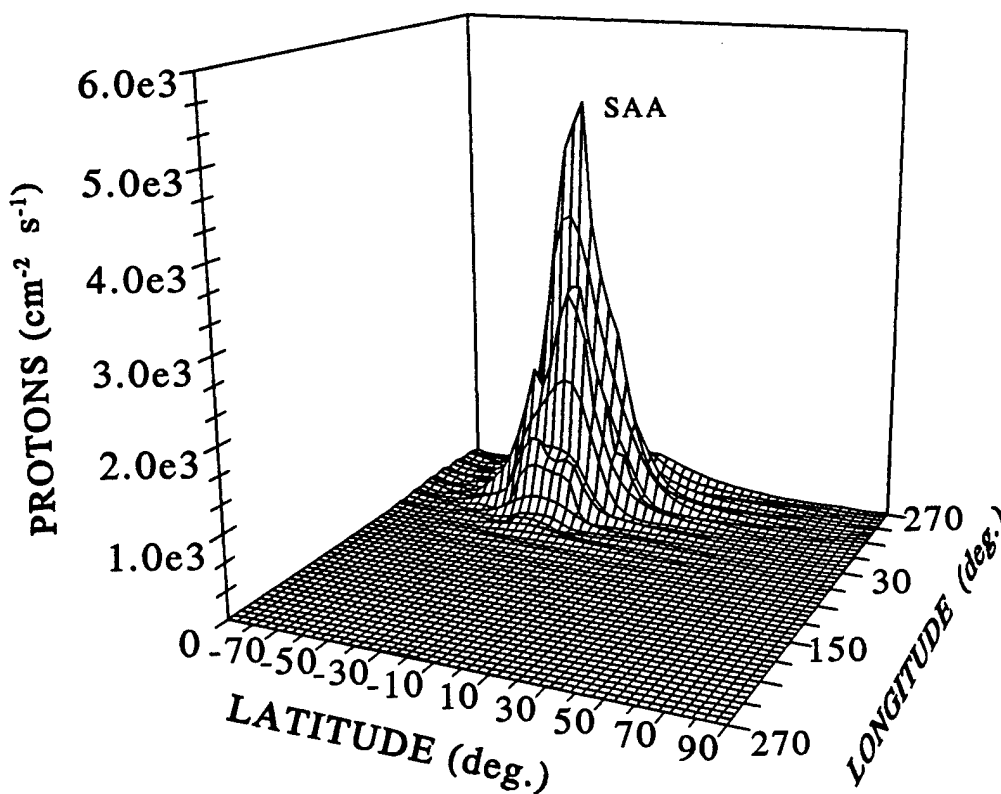


Figure 3. Spatial distribution of the trapped proton flux at the orbit of RADARSAT II.

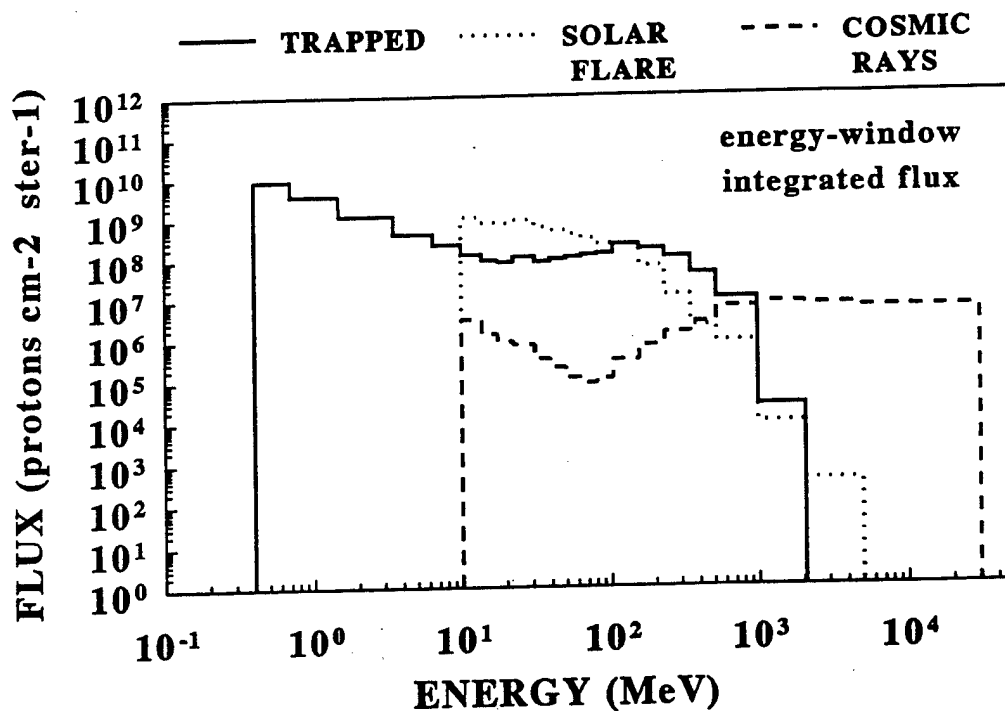


Figure 4. Mission- integrated estimation of trapped, solar flare and galactic cosmic ray proton fluence for RADARSAT II.

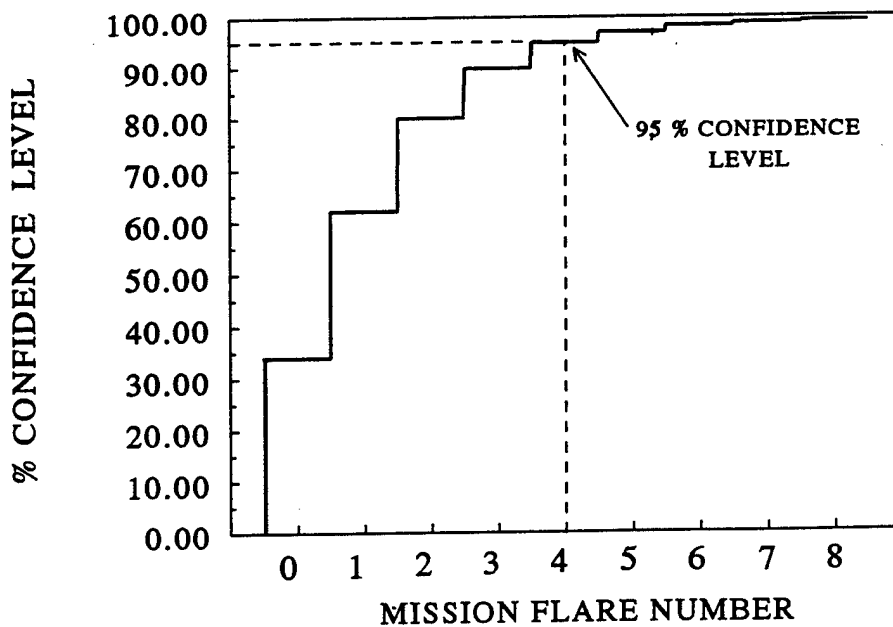


Figure 5. Confidence levels for predicting the occurrences of very large solar flares for the RADARSAT II mission.

Table 1. Mission-integrated trapped electron fluence for RADARSAT II

Energy (MeV) (el.cm ⁻² ster ⁻¹)		Energy (MeV) (el.cm ⁻² ster ⁻¹)	
.10-.20	2.75E12	1.30-1.40	6.93E9
.20-.30	1.13E12	1.40-1.50	5.80E9
.30-.40	4.76E11	1.50-1.60	4.96E9
.40-.50	2.15E11	1.60-1.70	4.17E9
.50-.60	7.91E10	1.70-1.80	3.51E9
.60-.70	5.31E10	1.80-1.90	2.95E9
.70-.80	3.28E10	1.90-2.00	2.49E9
.80-.90	2.14E10	2.00-2.25	4.52E9
.90-1.00	1.71E10	2.25-2.50	2.99E9
1.00-1.10	1.19E10	2.50-2.75	2.40E9
1.10-1.20	9.91E9	2.75-3.00	1.42E9
1.20-1.30	8.27E9	3.00-3.50	1.42E9

Table 2. Mission-integrated fluence of trapped, cosmic ray and solar flare protons for RADARSAT II.

Energy (MeV)	(protons cm ⁻² ster ⁻¹)			Total
	Trapped	Sol. Flare	Cos. Rays	
.40-.70	8.85E9	-	-	8.85E9
.70-1.5	3.71E9	-	-	3.71E9
1.5-3.5	1.20E9	-	-	1.20E9
3.5-6.5	4.20E8	-	-	4.20E8
6.5-10.0	2.24E8	-	-	2.24E8
10.0-13.8	1.26E8	1.07E9	3.20E6	1.20E9
13.8-17.6	9.02E7	7.82E8	1.37E6	8.74E8
17.6-22.4	8.15E7	7.34E8	8.97E5	8.17E8
22.4-31.0	1.08E8	8.93E8	7.63E5	1.00E9
31.0-39.4	8.18E7	5.70E8	3.39E5	6.52E8
39.4-50.2	9.39E7	4.90E8	2.07E5	5.84E8
50.2-64.0	1.05E8	3.95E8	1.15E5	5.00E8
64.0-81.5	1.17E8	3.01E8	8.44E4	4.18E8
81.5-104	1.28E8	2.18E8	1.05E5	3.45E8
104-156	2.12E8	2.10E9	3.01E5	4.22E8
156-233	1.66E8	6.19E7	7.02E5	2.29E8
233-349	1.01E8	1.16E7	1.43E6	1.14E8
349-522	3.95E7	2.05E6	2.45E6	4.40E7
522-995	9.70E6	8.83E5	5.86E6	1.65E7
995-2058	2.38E4	8.96E3	7.24E6	7.27E6
2058-5000	-	3.52E2	6.56E6	6.56E6
5000-3.0E4	-	-	5.54E6	5.54E6

4.3 HEAVY IONS

For heavy ions, two cases were considered, namely full ionization of solar-flare heavy ions and partial ionization. Measurements have shown⁽¹⁰⁾ that solar flare components are not fully ionized since they have not transversed as much matter as their galactic cosmic ray counterparts before reaching the Earth. Using the CREME model, this effect was modelled by including or excluding geomagnetic shielding. The effect of full versus partial ionization on the spectra of He, O and Fe ions is shown in Figures 6 and 7. In both figures, the solar flare protons are shown for comparison purpose as this flux is the same for both cases.

For energy dose deposition due to heavy ions, He ions have been considered. Two He spectra have been considered, one with a fully ionized solar flare component and one with a partially ionized solar flare component. Both spectra also contain fully ionized galactic cosmic ray component. Their binned energy spectra are given in Table 3.

Table 3. Mission-integrated flux of He ions for fully and partially ionized cases.

Energy (MeV)	Flux (He cm ⁻² ster ⁻¹)	
	Fully ionized	Partially ionized
45.0	3.404E7	1.756E8
57.4	3.080E7	1.644E8
73.0	3.136E7	1.504E8
93.5	2.896E7	1.340E8
128	4.120E7	1.816E8
190	3.072E7	1.284E8
283	2.016E7	1.472E8
423	1.128E7	4.200E7
680	4.800E6	1.800E7
1285	3.712E5	1.236E6
2700	5.142E4	1.072E5

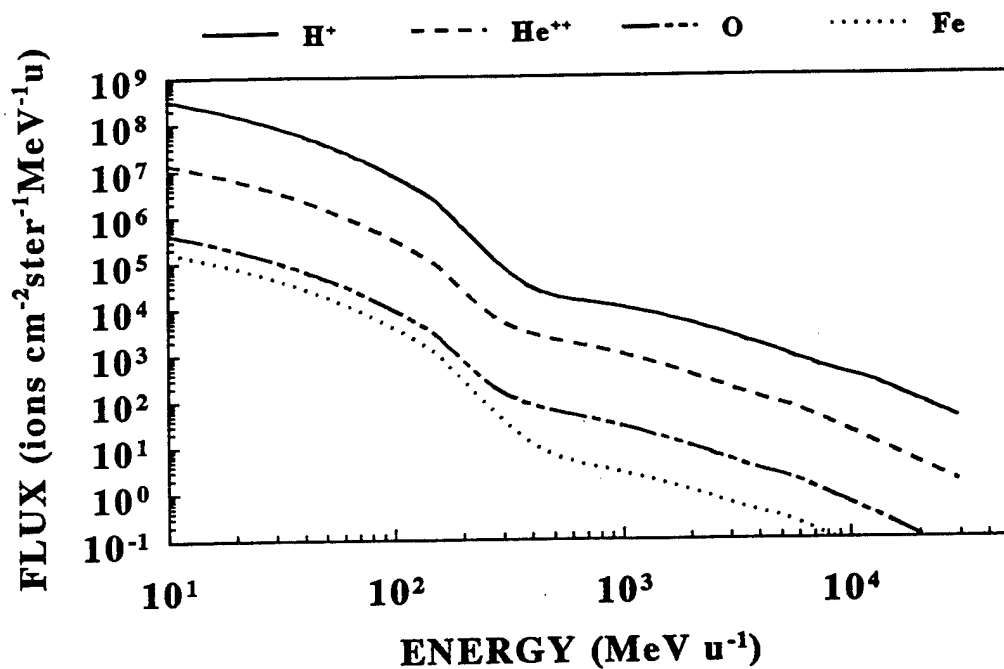


Figure 6. Mission-integrated differential spectra of He, O and Fe ions for RADARSAT II - full ionization case.

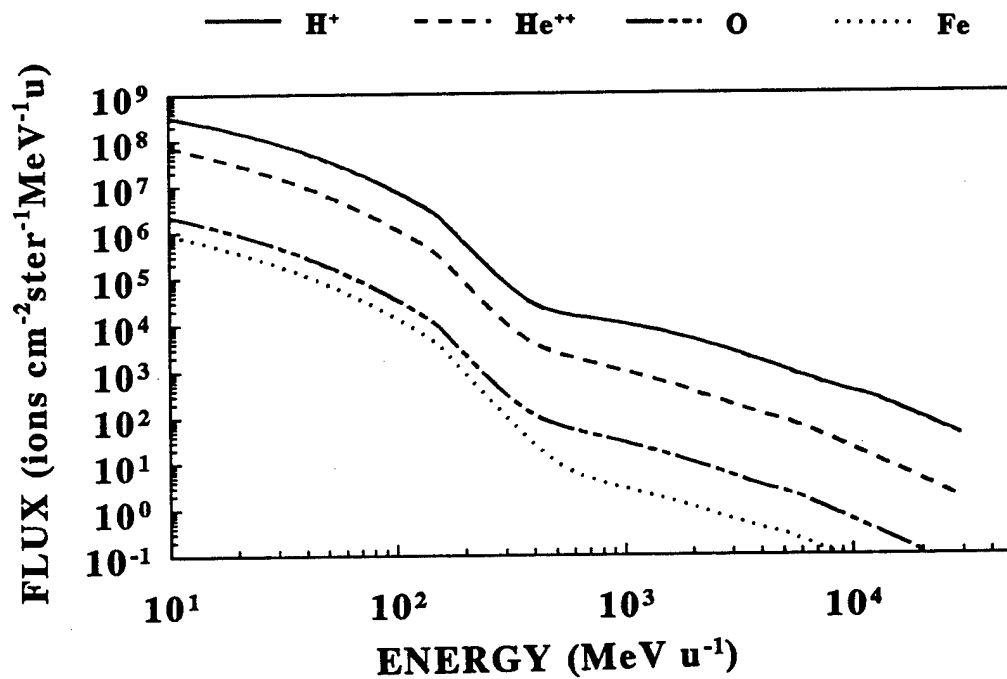


Figure 7. Mission-integrated differential spectra of He, O and Fe ions for RADARSAT II - partial ionization case.

5. MISSION-DOSE DETERMINATION

5.1 ELECTRON DEPTH/DOSE DISTRIBUTION

The TIGER (one-dimensional) code was used to simulate a 2π isotropic flux of electrons incident on a semi-infinite plane of aluminum (max thickness 3.5 cm). The absorbed dose (rad(Si)) was determined as a function of the depth of the aluminum shielding.

The trapped electron energy spectrum, determined via AE8, spanned the energy range of 0.1 MeV to 3.5 MeV. The energy binning selected for use in the AE8 flux determination and the ITS simulations is given in Table 1. In order to improve the computational efficiency of the Monte Carlo simulation, the electron energy spectrum (given in Table 1) was divided into 3 energy regions (while maintaining the same energy binning) and a TIGER simulation was conducted for each energy region. The energy regions selected were;

- region 1: 0.1 MeV - 0.4 MeV, 3 energy bins
- region 2: 0.4 MeV - 1.0 MeV, 6 energy bins
- region 3: 1.0 MeV - 3.5 MeV, 15 energy bins

It should be noted that this yields identical results to the case of running a single Monte Carlo simulation which encompasses the entire energy range of 0.1 MeV to 3.5 MeV.

The results of the three Monte Carlo simulations were combined to yield a single depth/dose curve by weighting each of the depth/dose curves for three energy regions by their respective flux contributions. It should be noted that only 50% of the 4π isotropic flux (determined via AE8) contributes to the absorbed dose for the semi-infinite plane configuration.

The depth dose curve for electrons, shown in Figure 8, illustrates the results of the analysis. The solid curve represents the total mission dose (rad(Si)) due to electrons in the energy range of 0.1 MeV to 3.5 MeV. The dose values shown represent the dose contribution by both electrons and Bremsstrahlung. The continuous-slowing-down approximation (CSDA) range of a 3.5 MeV electron in aluminum is approximately 0.8 cm; the depth/dose data reflects this as the depth/dose gradient becomes relatively constant beyond 0.8 cm Al thickness. The dose contribution beyond 0.8 cm Al shield thickness is, therefore, due to Bremsstrahlung radiation only. The depth/dose data shown in Figure 8 is also presented in Table 4; the dose is given as a function of Al shield depth for 1 mm depth increments.

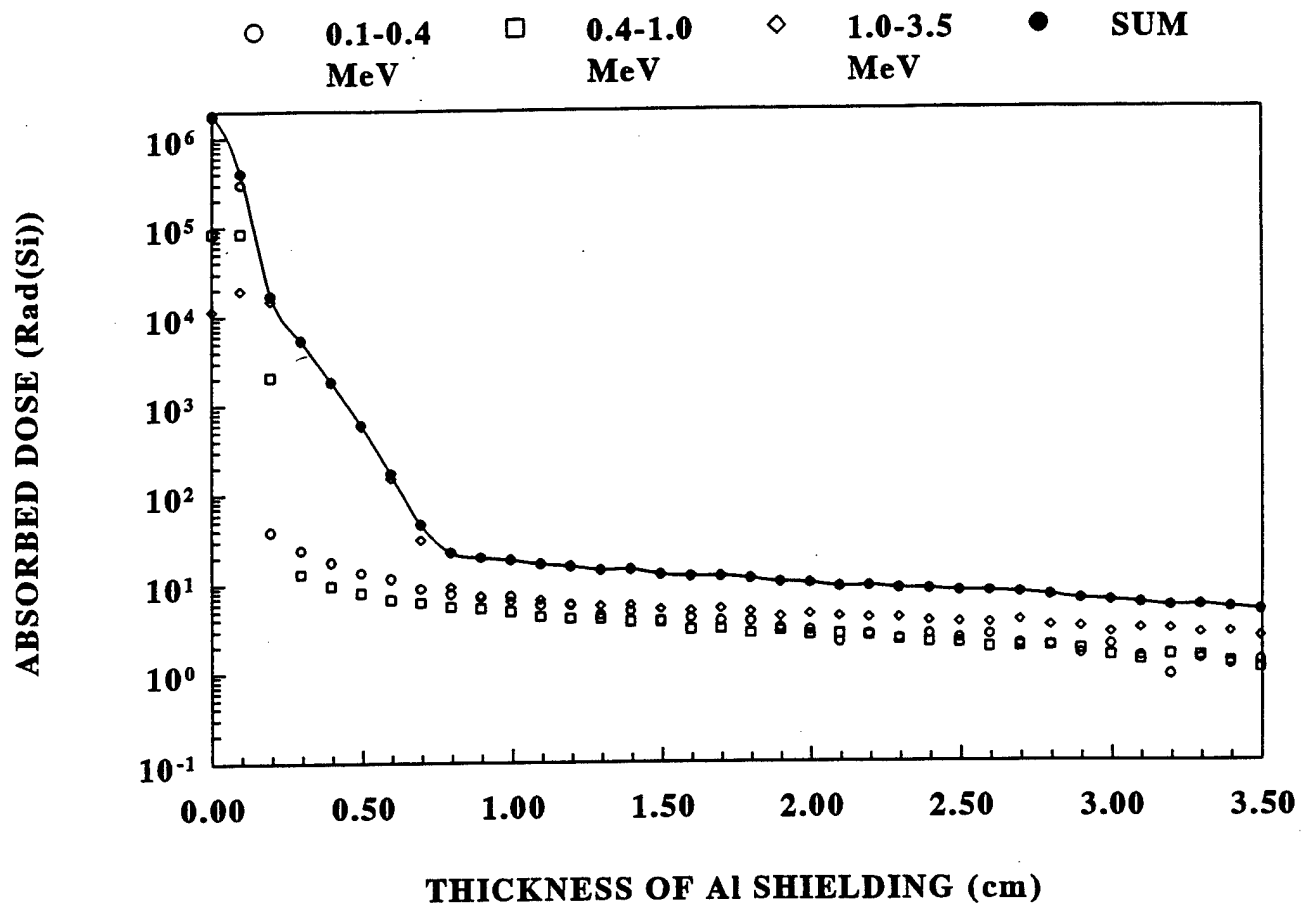


Figure 8. Mission depth/dose profile for electrons in aluminum as a function of Al shielding depth, for RADARSAT II.

5.2 PROTON CONTRIBUTION TO TOTAL MISSION DOSE

The energy windows and the "average" proton energy (i.e. fluence-weighted proton energy for each window) used in the PROTDOS simulations are shown in Table 5. This table is applicable for the PROTDOS estimates of the proton dose due to trapped, cosmic ray and solar flare protons. The corresponding fluence values, shown in Table 2, were also used, after multiplication by 2π (since PROTDOS models a 2π isotropic ion flux incident on a semi-infinite plane geometry).

To illustrate the output of the TRIM simulations required for use by PROTDOS (see Figure 9), the TRIM output for 3 angles (out of a total of 10 angles) of incidence for 128 MeV protons in aluminum are graphically shown. For 0 degrees angle of incidence, the proton passes through the 3 cm maximum thickness of

Table 4. RADARSAT II total mission dose (5.25 years), as a function of aluminum shielding thickness, due to trapped electrons.

5.25 YEAR MISSION DOSE DUE TO ELECTRONS RADARSAT II				
Al SHIELD THICKNESS (cm)	0.1 - 0.4 MeV ELECTRON DOSE (rad(Si))	0.4 - 1.0 MeV ELECTRON DOSE (rad(Si))	1.0 - 3.5 MeV ELECTRON DOSE (rad(Si))	TOTAL ELECTRON DOSE (rad(Si))
0.0	1.7454E+06	8.4715E+04	1.1407E+04	1.8415E+06
0.1	2.9982E+05	8.4433E+04	1.9336E+04	4.0358E+05
0.2	3.8688E+01	2.0818E+03	1.4943E+04	1.7063E+04
0.3	2.4089E+01	1.3105E+01	5.3100E+03	5.3472E+03
0.4	1.7762E+01	9.6801E+00	1.8026E+03	1.8300E+03
0.5	1.3519E+01	8.0103E+00	5.7527E+02	5.9680E+02
0.6	1.1628E+01	6.6887E+00	1.5031E+02	1.6862E+02
0.7	8.9469E+00	6.2090E+00	3.1252E+01	4.6407E+01
0.8	7.7807E+00	5.5391E+00	9.2637E+00	2.2584E+01
0.9	7.1206E+00	5.3110E+00	7.3361E+00	1.9768E+01
1.0	7.2498E+00	4.9049E+00	6.4133E+00	1.8568E+01
1.1	5.7566E+00	4.2432E+00	6.5810E+00	1.6581E+01
1.2	5.7819E+00	4.0542E+00	5.8282E+00	1.5664E+01
1.3	4.4395E+00	4.0199E+00	5.6079E+00	1.4067E+01
1.4	4.8481E+00	3.6908E+00	5.7293E+00	1.4268E+01
1.5	3.7645E+00	3.7054E+00	5.1126E+00	1.2583E+01
1.6	4.0527E+00	3.0417E+00	4.9210E+00	1.2015E+01
1.7	3.7626E+00	3.0508E+00	5.1330E+00	1.1946E+01
1.8	3.7114E+00	2.7282E+00	4.7398E+00	1.1179E+01
1.9	3.1320E+00	2.9058E+00	4.1254E+00	1.0163E+01
2.0	2.9424E+00	2.5908E+00	4.4112E+00	9.9444E+00
2.1	2.1513E+00	2.6415E+00	4.1803E+00	8.9731E+00
2.2	2.6180E+00	2.5511E+00	4.0111E+00	9.1801E+00
2.3	2.3421E+00	2.2689E+00	3.9923E+00	8.6033E+00
2.4	2.6367E+00	2.1478E+00	3.7084E+00	8.4929E+00
2.5	2.3794E+00	2.1088E+00	3.5772E+00	8.0654E+00
2.6	2.5844E+00	1.8738E+00	3.5248E+00	7.9830E+00
2.7	2.0538E+00	1.8990E+00	3.7366E+00	7.6893E+00
2.8	1.9524E+00	1.9156E+00	3.2602E+00	7.1282E+00
2.9	1.5658E+00	1.7593E+00	3.1394E+00	6.4645E+00
3.0	1.9714E+00	1.4918E+00	2.7073E+00	6.1705E+00

Table 5. Proton energy windows and the corresponding "average" proton energy used in PROTDOS simulation of proton depth/dose profiles as a function of depth of aluminum shielding.

Proton Energy Window (MeV)	Average Proton Energy for Window (MeV)	Proton Energy Window (MeV)	Average Proton Energy for Window (MeV)
0.40 - 0.70	0.55	50.2 - 64.0	56.0
0.70 - 1.50	1.10	64.0 - 81.5	70.5
1.50 - 3.50	2.50	81.5 - 104	93.4
3.50 - 6.50	5.00	104 - 156	128
6.50 - 10.0	8.25	156 - 233	190
10.0 - 13.8	11.4	233 - 349	280
13.8 - 17.6	15.3	349 - 522	397
17.6 - 22.4	19.6	522 - 995	775
22.4 - 31.0	25.8	995 - 2058	1415
31.0 - 39.4	34.8	2058 - 5000	3400
39.4 - 50.2	43.6	5000 - 3.0E+04	1.0E+04

aluminum shielding (the range of a 128 MeV proton in aluminum is approximately 5.8 cm). The energy deposited is relatively uniform as a function of depth. For 70 and 85 degrees angle of incidence, the proton is stopped completely within the aluminum shielding. The peak of the energy deposition profile becomes more pronounced and is located at progressively shallower depth as the angle of incidence increases.

Another useful output of TRIM is the Table of the proton range in aluminum, shown graphically in Figure 10. This data permits the analyst to determine, for a given shielding configuration (i.e. thickness of aluminum), what the lower limit is for the proton energy that can penetrate a given shielding thickness. For specific cases, this can minimize the amount of computation required, by allowing the analyst to ignore proton energies below the lower limit.

The results of the PROTDOS simulations are summarized in Table 6 and illustrated graphically in Figure 11. Here the contribution of the three groups of protons (solar flare, cosmic ray and trapped protons) to the mission dose, as well as the total mission proton dose (5.25 year mission duration) are given.

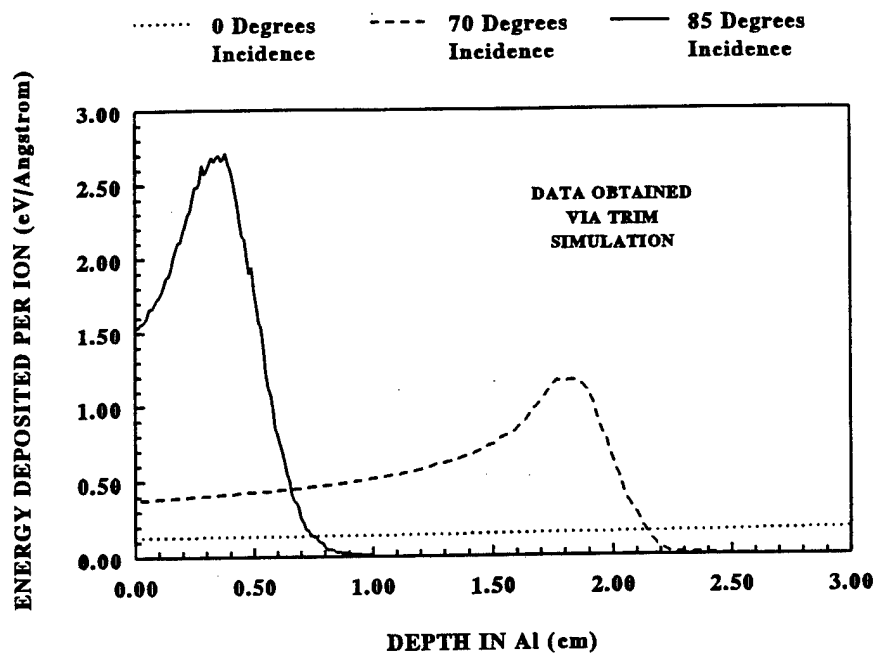


Figure 9. Graphical representation of TRIM simulation output for energy deposition by 128 MeV protons, as a function of depth of aluminum, at 0 degree, 70 degree and 85 degree angles of incidence.

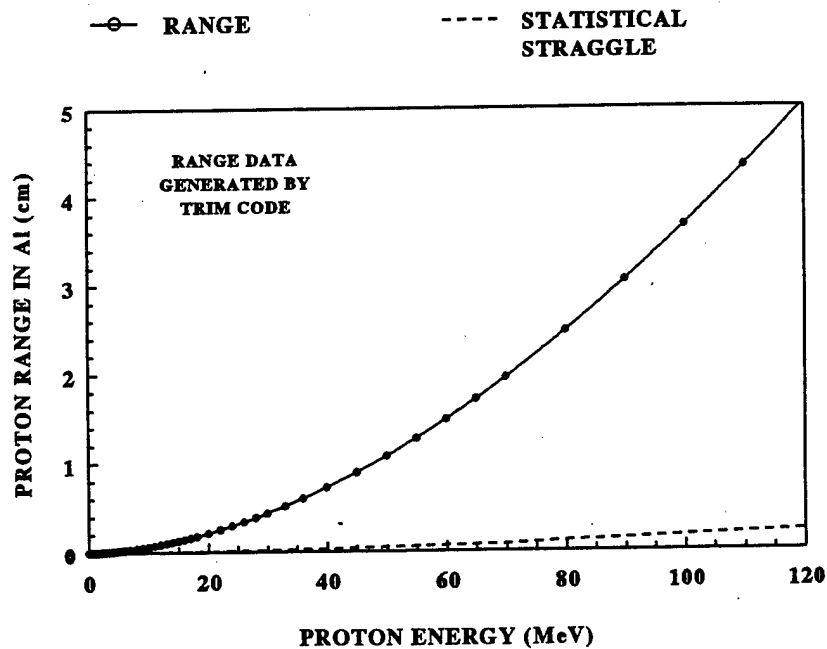


Figure 10. TRIM generated proton range in aluminum data.

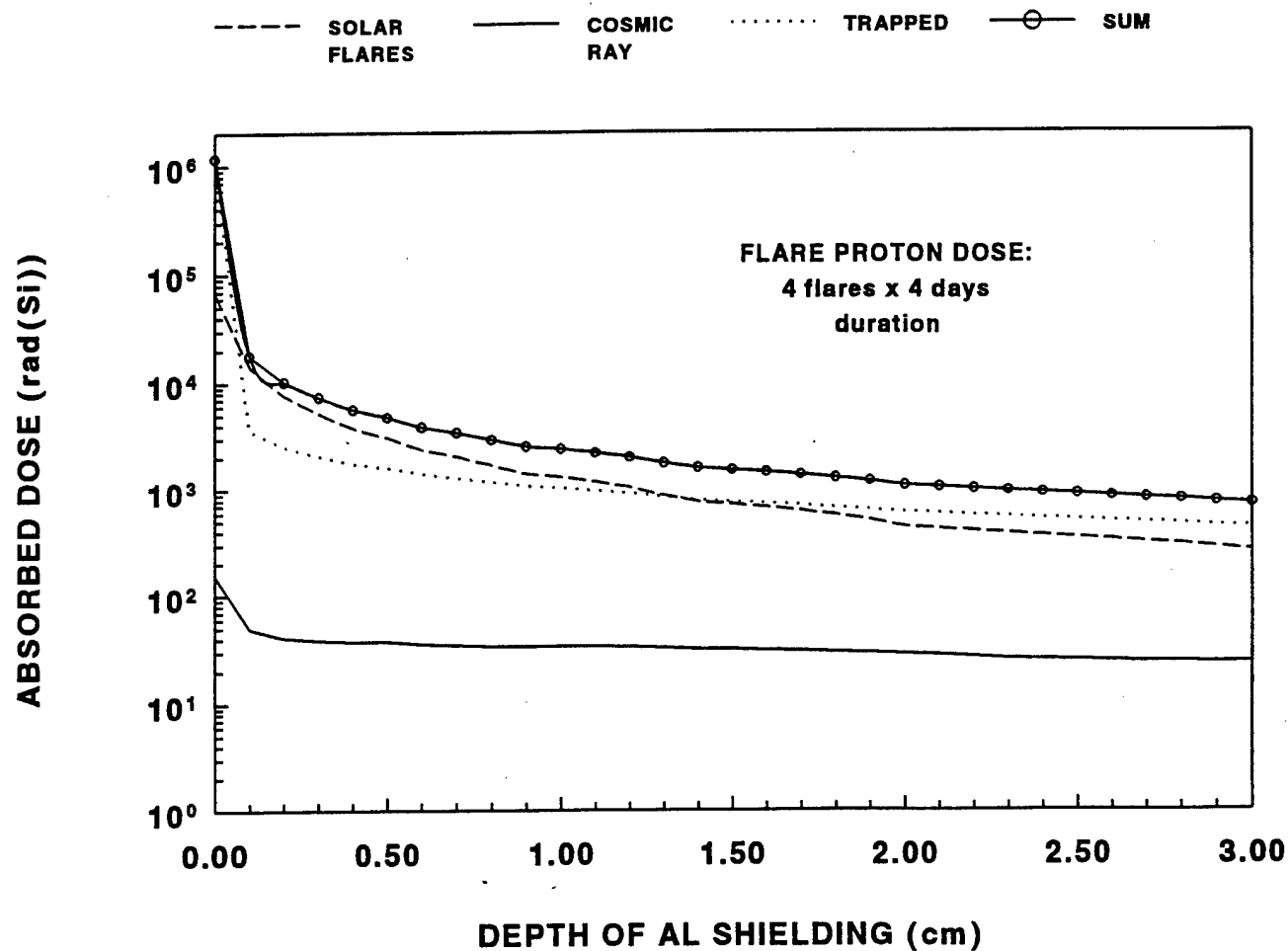


Figure 11. RADARSAT II mission proton dose estimates, as a function of depth of Al shielding.

For the case of 0 cm Al shielding, as expected the trapped protons dominate the proton dose, as they are the most abundant at relatively low proton energies (<10 MeV) and experience the largest dE/dx at shallow depths (for protons in aluminum, the maximum dE/dx is reached at a proton energy of approximately 65 keV and decreases for higher proton energies. From 0.10 cm Al to about 1.3 cm Al, the dose due to solar flares dominates over the trapped proton dose, due to the larger fluence below 156 MeV. Above this energy, the trapped flux dominates and this is reflected in a higher dose contribution for trapped protons for shielding thickness greater than about 1.3 cm of Al. The cosmic ray contribution to the total proton dose is relatively small (compared to either the solar flare or trapped proton dose) due to the commensurate low fluence throughout the full proton energy range.

Table 6. Radarsat II total mission dose (5.25 years), as a function of aluminum shielding thickness, due to protons.

5.25 YEAR MISSION DOSE DUE TO PROTONS RADARSAT II				
Al Shield Thickness (cm)	Solar Flare Dose (rad(Si))	Cosmic Ray Dose (rad(Si))	Trapped Proton Dose (rad(Si))	Total Proton Dose (rad(Si))
0.0	6.9138E+04	1.5427E+02	1.1052E+06	1.1745E+06
0.1	1.4285E+04	4.9539E+01	3.6622E+03	1.7997E+04
0.2	7.6664E+03	4.1215E+01	2.5652E+03	1.0273E+04
0.3	5.2830E+03	3.8633E+01	2.0926E+03	7.4142E+03
0.4	3.8115E+03	3.7887E+01	1.7830E+03	5.6325E+03
0.5	3.1123E+03	3.7676E+01	1.6031E+03	4.7530E+03
0.6	2.3818E+03	3.6059E+01	1.4233E+03	3.8411E+03
0.7	2.0687E+03	3.4667E+01	1.3039E+03	3.4073E+03
0.8	1.7033E+03	3.3761E+01	1.1799E+03	2.9170E+03
0.9	1.4114E+03	3.3793E+01	1.0875E+03	2.5326E+03
1.0	1.3110E+03	3.3795E+01	1.0445E+03	2.3893E+03
1.1	1.1743E+03	3.3717E+01	9.8139E+02	2.1894E+03
1.2	1.0402E+03	3.3385E+01	9.1814E+02	1.9917E+03
1.3	8.7108E+02	3.2516E+01	8.4705E+02	1.7506E+03
1.4	7.6752E+02	3.1885E+01	7.9591E+02	1.5953E+03
1.5	7.2074E+02	3.1503E+01	7.6504E+02	1.5173E+03
1.6	6.7640E+02	3.0947E+01	7.3249E+02	1.4398E+03
1.7	6.2586E+02	3.0508E+01	7.0212E+02	1.3585E+03
1.8	5.6593E+02	2.9530E+01	6.6804E+02	1.2635E+03
1.9	5.1390E+02	2.9093E+01	6.4260E+02	1.1856E+03
2.0	4.3552E+02	2.8442E+01	6.0520E+02	1.0692E+03
2.1	4.1799E+02	2.7603E+01	5.8769E+02	1.0333E+03
2.2	3.9686E+02	2.6696E+01	5.6584E+02	9.8939E+02
2.3	3.7998E+02	2.5606E+01	5.4874E+02	9.5433E+02
2.4	3.6260E+02	2.5117E+01	5.3061E+02	9.1833E+02
2.5	3.4833E+02	2.4703E+01	5.1506E+02	8.8809E+02
2.6	3.2732E+02	2.4423E+01	4.9456E+02	8.4630E+02
2.7	3.1136E+02	2.4261E+01	4.8129E+02	8.1691E+02
2.8	2.9815E+02	2.4017E+01	4.6855E+02	7.9072E+02
2.9	2.7848E+02	2.3845E+01	4.5134E+02	7.5366E+02
3.0	2.6053E+02	2.3715E+01	4.3564E+02	7.1989E+02

NOTES:

1. The FLARE DOSE represents the summation of the proton dose due to 4 solar flares. Each flare is assumed to have a 4 day duration.

5.3 He CONTRIBUTION TO TOTAL MISSION DOSE

The depth/dose curve for He ions (for both fully ionized and partially ionized He ions) were obtained in a similar fashion to that for protons, using TRIM and PROTDISE. The He ion energy and the corresponding mission fluence from Table III were input into PROTDISE, after the fluence values had been multiplied by 2π steradians.

The results of the PROTDISE simulations are presented in Table 7 and are also shown graphically in Figure 12. The partially ionized He ions contribute a larger dose at any depth of Al shielding due to the larger fluence for all He ion energies. Relative to protons at a given energy, He ions have a shorter range and, therefore, a correspondingly larger dE/dx .

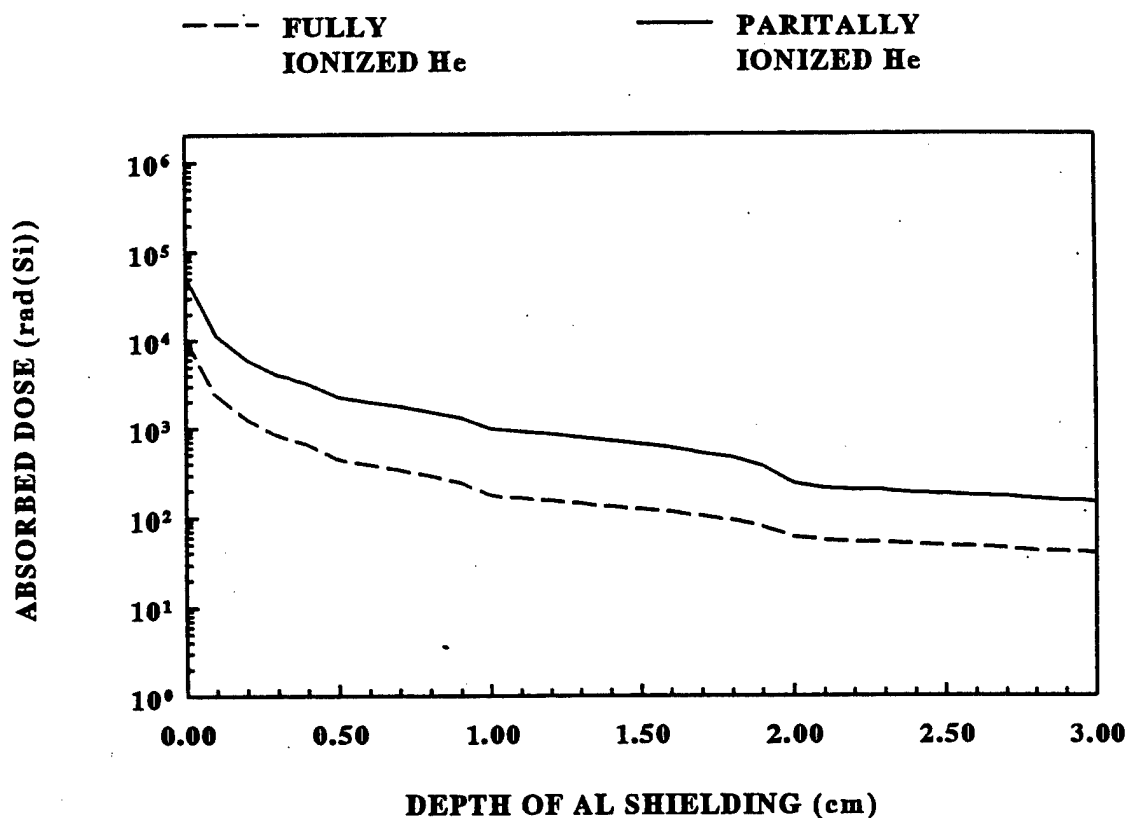


Figure 12. RADARSAT II mission He ion (alpha particles) dose estimates, as a function of Al shielding thickness.

Table 7. RADARSAT II total mission dose (5.25 years), as a function of aluminum shielding thickness, due to fully ionized and partially ionized He ions.

5.25 YEAR MISSION DOSE DUE TO He IONS RADARSAT II		
Depth Al Shield (cm)	Fully Ionized He Dose (rad(Si))	Partially Ionized He Dose (rad(Si))
0.0	1.0915E+04	5.3959E+04
0.1	2.3883E+03	1.1439E+04
0.2	1.2719E+03	6.0716E+03
0.3	8.4369E+02	4.0753E+03
0.4	6.5622E+02	3.2157E+03
0.5	4.4134E+02	2.2369E+03
0.6	3.8651E+02	1.9718E+03
0.7	3.4014E+02	1.7540E+03
0.8	2.9459E+02	1.5261E+03
0.9	2.4499E+02	1.2924E+03
1.0	1.7651E+02	9.8498E+02
1.1	1.6603E+02	9.2057E+02
1.2	1.5448E+02	8.4796E+02
1.3	1.4470E+02	7.8855E+02
1.4	1.3341E+02	7.1377E+02
1.5	1.2402E+02	6.5553E+02
1.6	1.1563E+02	6.0262E+02
1.7	1.0270E+02	5.1570E+02
1.8	9.3602E+01	4.5950E+02
1.9	8.0733E+01	3.7266E+02
2.0	6.1227E+01	2.4118E+02
2.1	5.5922E+01	2.0789E+02
2.2	5.4208E+01	2.0150E+02
2.3	5.2611E+01	1.9554E+02
2.4	5.0029E+01	1.8593E+02
2.5	4.8527E+01	1.8034E+02
2.6	4.6712E+01	1.7359E+02
2.7	4.5408E+01	1.6874E+02
2.8	4.2647E+01	1.5845E+02
2.9	4.0827E+01	1.5168E+02
3.0	3.9276E+01	1.4590E+02

6. SUMMARY

The proposed launch date and the duration of the mission preclude RADARSAT II being in orbit during the solar maximum of #23 solar cycle. The radiation environment for this epoch has been estimated utilizing AP-8, AE-8 and CREME models. Data processing from these models involved unit conversions to make the radiation data from the CREME model compatible with the AP-8/AE-8 models. All the radiation components of the environment with the exception of anomalously large solar flares have been integrated over 1917.25 mission days. The large solar flare components of the radiation environment have been integrated over 16 mission solar-flare days. This was then followed by additional flux integration to make the data compatible with the input requirements of the radiation transport codes. This data manipulation involved the generation of appropriate energy windows followed by integration of the differential flux over the energy window width. This was accomplished by fitting a 3rd order polynomial into individual differential data points of each energy bin, followed by analytical integration using the coefficients of fitted polynomials. The window energy represented in the final data corresponds to the average flux of the window and not the window centre.

The electron flux over the mission was estimated using AE-8MAX module of the AE-8 model with the results presented in section 4.1 of this report. It was determined that most of the dose deposition due to electrons is associated with the SAA region. Some dose deposition will also occur in auroral zones, predominantly during magnetospheric storms.

The proton environment, presented in section 4.2, was assembled from trapped protons, galactic cosmic ray protons and protons of solar flare origin. For the trapped protons, just as for electrons, the major contribution to the total dose deposited by protons occurs in the SAA region. King's model was used to estimate with 95% confidence the contribution of solar flare protons to the total dose.

The CREME model was also used to estimate the flux of He, O and Fe ions. The sources of these ions are solar flares and galactic cosmic rays. Total and partial ionization of these ions was considered by inclusion and exclusion of the geomagnetic shielding effect. The results were presented in section 4.3. The mission-integrated energy-binned flux of He ions in Table 3 was used for dose deposition determination.

The depth/dose profiles for electrons, protons and He ions were calculated using the ITS codes for electrons and the combination of TRIM and PROTDose codes for protons and He ions. It should be noted that the use of a semi-infinite plane geometry results in an overestimate of the dose delivered to a semiconductor device, due to the finite lateral extent of the semiconductor die. This geometry precludes the use of a 2π isotropic fluence. From the perspective of the incident

fluence, this technique results in an underestimate in the dose, because the fluence from the backside of the shielding is deemed as non-contributing to the total dose.

It should also be noted that in all of the simulations conducted in this study, the effect of device packaging on the absorbed dose has *not* been taken into account. Although the energy loss in packaging material by high energy protons (or He ions) is insignificant, even when moderate aluminum shielding is provided, this is not the case at the low end of the energy spectrum. Low energy protons can be completely stopped within the ceramic or plastic device packaging and for the case of 0 mm Al shielding, the dose is probably grossly overestimated for protons and He ions. [To a lesser extent, the same argument is likely applicable for low energy electrons.] This overestimate occurs because the largest particle fluence occurs at the lowest particle energy ranges and it is this energy range which dominates the absorbed dose for minimal shielding (i.e. 0 mm Al).

As an example of the dose overestimate which can result from neglecting the effect of device packaging, consider a semiconductor device packaged in an ceramic (Al_2O_3) package, with a typical lid thickness of approximately 0.8 mm. At normal incidence, the minimum proton energy that can penetrate the top of the package and reach the semiconductor die is approximately 15 MeV; for He ions (alphas), 60 MeV is required. For electrons, the minimum electron energy that can penetrate through the package is approximately 0.65 MeV, based upon the CSDA range. In the case of protons, a significant fluence is present below 15 MeV, which greatly contributes to the absorbed dose for 0 mm shielding. For He ions, there is also a significant fluence below 60 MeV. If the fluences for these two components were properly accounted for, in terms of the effect of device packaging, the corresponding depth/dose profiles would be significantly altered (i.e. reduced) for moderate shielding thicknesses. In the case of electrons, up to 0.65 MeV electrons can be stopped within the ceramic package, however, secondary electrons and Bremsstrahlung generated within the ceramic lid can feasibly reach the semiconductor die and contribute to the absorbed dose. Only a Monte Carlo analysis can fully estimate this effect.

The effect of packaging materials on the absorbed dose due to protons and alpha particles (He ions) can be investigated upon modification of the PROTDose code, however, estimates of these effects can be performed by simply assigning a low energy cut-off to the appropriate particle energy spectrum. This low energy cut-off is particle and device package (i.e. thickness, composition and geometry) dependent. The effect of packaging materials on the electron dose can be easily modelled by simply modifying the input file problem description in the ITS codes. No change is required in the input electron source spectrum. With code modification, PROTDose also could be used to investigate the effect of finite device dimensions on the absorbed dose due to light and heavy ions.

7. REFERENCES

1. Tranquille, C. and E.J. Daly, "Evaluation of Solar-Proton Models for ESA Missions", ESA Journal, Vol. 16, 1992.
2. ESA, "The Radiation Design Handbook", ESA PSS-01-609 Issue 1, May 1993.
3. Vette, I.J., "The AE-8 Trapped Electron Model Environment", NSSDC 91-24, 1991
4. Sawyer, M.D. and I. J. Vette, "AP-8 Trapped Proton Environment for Solar maximum and Solar Minimum", NSSDC/WDC-A-R&S 76-06, National Space Science data Center, NASA, 1976.
5. Adams, J.H., "Cosmic Ray Effects on Microelectronics (Part IV)", NRL Memorandum Report 5901, 1986.
6. Engelmann, J.J., P. Goret, E. Juliusson, L. Koch-Miramond, P. Masse, A. Soutoul, P. Byrnek, N. Lund, B. Peters, I.L. Rassmussen, M. Rotenberg and N. J. Westergaard, "Elemental Composition of Cosmic rays from Be to Ni as Measured by the French-danish Instrument on HEAO-3", Proceedings of the 18th Inter. Cosmic ray Conf., Vol. 2, 17-20, Bangalore, India, 1983.
7. King, J.H., "Solar Proton Fluences for 1977-1983 Space Missions", J. Spacecraft, Vol. 11, p. 401.
8. S. Seltzer, "Shieldose: A Computer Code for Space-Shielding Radiation Dose Calculations", NBS Technical Note 1116, May 1980.
9. J.F. Ziegler, J.P. Biersack, U. Littmark, "The Stopping and Range of Ions in Solids", Vol. 1, Pergamon Press, New York, 1985.
10. Gloecker, G., H. Weiss, D. Hovestadt, F.M. Ipavich, B. Klecker, L.A. Fisk, M. Scholer, C.Y. Fan and J.J. O'Gallagher, "Observations of the Ionization States of Energetic particles Accelerated in Solar Flares", Proc. of the 17th Intl. Cosmic ray Conf., Paris, Vol. 3, 136-9, 1981.
11. Anderson, B.J., ed., "Natural Orbital Environment Guideline for Use in Aerospace Vehicle Development" NASA Technical Memorandum 4527 (1994).

UNCLASSIFIED

SECURITY CLASSIFICATION OF FORM
(highest classification of Title, Abstract, Keywords)

DOCUMENT CONTROL DATA

(Security classification of title, body of abstract and indexing annotation must be entered when the overall document is classified)

1. ORIGINATOR (the name and address of the organization preparing the document. Organizations for whom the document was prepared, e.g. Establishment sponsoring a contractor's report, or tasking agency, are entered in section 8.) Defence Research Establishment Ottawa Ottawa, Ontario K1A 0Z4		2. SECURITY CLASSIFICATION (overall security classification of the document including special warning terms if applicable) UNCLASSIFIED
3. TITLE (the complete document title as indicated on the title page. Its classification should be indicated by the appropriate abbreviation (S,C or U) in parentheses after the title.) Space Radiation Environment Estimation for RADARSAT II (U)		
4. AUTHORS (Last name, first name, middle initial) Varga L., Pepper G.T. and Woods P.		
5. DATE OF PUBLICATION (month and year of publication of document) 09/96	6a. NO. OF PAGES (total containing information. Include Annexes, Appendices, etc.) 27	6b. NO. OF REFS (total cited in document) 11
7. DESCRIPTIVE NOTES (the category of the document, e.g. technical report, technical note or memorandum. If appropriate, enter the type of report, e.g. interim, progress, summary, annual or final. Give the inclusive dates when a specific reporting period is covered.) DREO Report		
8. SPONSORING ACTIVITY (the name of the department project office or laboratory sponsoring the research and development. Include the address.) Defence Research Establishment Ottawa Ottawa, Ontario, K1A 0Z4		
9a. PROJECT OR GRANT NO. (if appropriate, the applicable research and development project or grant number under which the document was written. Please specify whether project or grant) 1410SS-05E03	9b. CONTRACT NO. (if appropriate, the applicable number under which the document was written)	
10a. ORIGINATOR'S DOCUMENT NUMBER (the official document number by which the document is identified by the originating activity. This number must be unique to this document.) DREO Report 1292	10b. OTHER DOCUMENT NOS. (Any other numbers which may be assigned this document either by the originator or by the sponsor)	
11. DOCUMENT AVAILABILITY (any limitations on further dissemination of the document, other than those imposed by security classification) <input checked="" type="checkbox"/> (X) Unlimited distribution <input type="checkbox"/> () Distribution limited to defence departments and defence contractors; further distribution only as approved <input type="checkbox"/> () Distribution limited to defence departments and Canadian defence contractors; further distribution only as approved <input type="checkbox"/> () Distribution limited to government departments and agencies; further distribution only as approved <input type="checkbox"/> () Distribution limited to defence departments; further distribution only as approved <input type="checkbox"/> () Other (please specify):		
12. DOCUMENT ANNOUNCEMENT (any limitation to the bibliographic announcement of this document. This will normally correspond to the Document Availability (11). however, where further distribution (beyond the audience specified in 11) is possible, a wider announcement audience may be selected.) Unlimited Announcement		

UNCLASSIFIED

SECURITY CLASSIFICATION OF FORM

RA.W (21 Dec 92)

UNCLASSIFIED

SECURITY CLASSIFICATION OF FORM

- 13. ABSTRACT** (a brief and factual summary of the document. It may also appear elsewhere in the body of the document itself. It is highly desirable that the abstract of classified documents be unclassified. Each paragraph of the abstract shall begin with an indication of the security classification of the information in the paragraph (unless the document itself is unclassified) represented as (S), (C), or (U). It is not necessary to include here abstracts in both official languages unless the text is bilingual).

Estimation of radiation environment for RADARSAT II satellite (to be launched in the fall 2000) is presented using industry-standard space radiation models CREME and AE8/AP8. Radiation transport Monte Carlo codes TRIM and ITS 3.0 Tiger were then subsequently used to calculate the total radiation dose that will be received by RADARSAT II during the planned 5.25 year mission.

- 14. KEYWORDS, DESCRIPTORS or IDENTIFIERS** (technically meaningful terms or short phrases that characterize a document and could be helpful in cataloguing the document. They should be selected so that no security classification is required. Identifiers, such as equipment model designation, trade name, military project code name, geographic location may also be included. If possible keywords should be selected from a published thesaurus. e.g. Thesaurus of Engineering and Scientific Terms (TEST) and that thesaurus-identified. If it is not possible to select indexing terms which are Unclassified, the classification of each should be indicated as with the title.)

Space Environment
Trapped Radiation
Cosmic Rays
Solar Flares
AE8
AP8
CREME
Monte Carlo
ITS
TRIM
Total Dose

UNCLASSIFIED

SECURITY CLASSIFICATION OF FORM